

Climatological Features of Winter Lightning Activity in the Coastal Area of Sea of Japan, Tohoku and Hokuriku District

TSURUSHIMA, Daiki / HONMA, Noriyasu / SAKAIDA, Kiyotaka

(出版者 / Publisher)

Japan Climatology Seminar

(雑誌名 / Journal or Publication Title)

Japanese progress in climatology / Japanese progress in climatology

(巻 / Volume)

2014

(開始ページ / Start Page)

38

(終了ページ / End Page)

44

(発行年 / Year)

2014-12

(URL)

<https://doi.org/10.15002/00010793>

Reprinted from *Quarterly Jour. of Geography*. Vol. 65-4, pp. 189~206, 2014.

Climatological Features of Winter Lightning Activity in the Coastal Area of Sea of Japan, Tohoku and Hokuriku District

Daiki TSURUSHIMA*, Kiyotaka SAKAIDA* and Noriyasu HONMA**

This research clarified some statistical features of winter lightning activity in the coastal areas of Sea of Japan based on observational data obtained by Lightning Location System (LLS) in Tohoku district. Analysis of data indicated that during the cold season, the highest lightning frequency was displayed in the late autumn (Oct-Nov), when intensive lightning activity occurred in the coastal areas of Aomori and Akita prefectures. In the mid-winter season (Dec-Jan), the region of intense lightning activity moved southward to Yamagata and Niigata prefectures. Lightning frequency in the late winter season (Feb-Mar) was the lowest, with the region of intense lightning activity moving northward to Yamagata and Akita prefectures. An examination of ERA-interim reanalysis data revealed that during lightning days, Tohoku and Hokuriku districts were located near the southern part of the cyclone passing over Sea of Japan. Moreover, seasonal variation of lightning frequency patterns might be related to the prevailing wind direction in the study area. In the late autumn season, the prevailing surface wind direction over Sea of Japan was west to southwest, which created a strong wind convergence zone near the coastal areas of Aomori and Akita prefectures. However, the convergence zone moved southward when the wind direction changed northward in the mid-winter season. During the late winter season, the changes in wind patterns caused the convergence zone to be again formed near Aomori and Akita prefectures. These results are consistent with the changes in lightning frequency pattern.

Key words : Tohoku district, Hokuriku district, Sea of Japan, Winter lightning, Lightning Location System (LLS), wind convergence

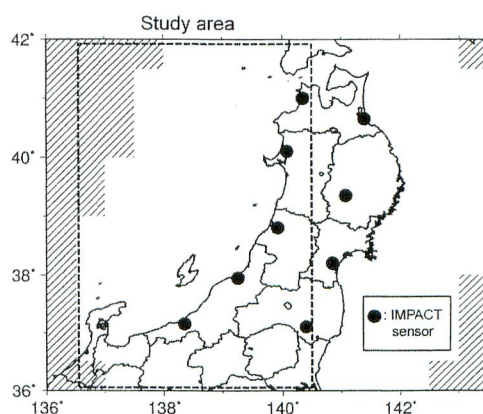


Fig. 1 Location of the study area (broken line) and the IMPACT sensors. Meshed area indicates undetected zones of lightning discharge with absolute peak currents below 10 kA.

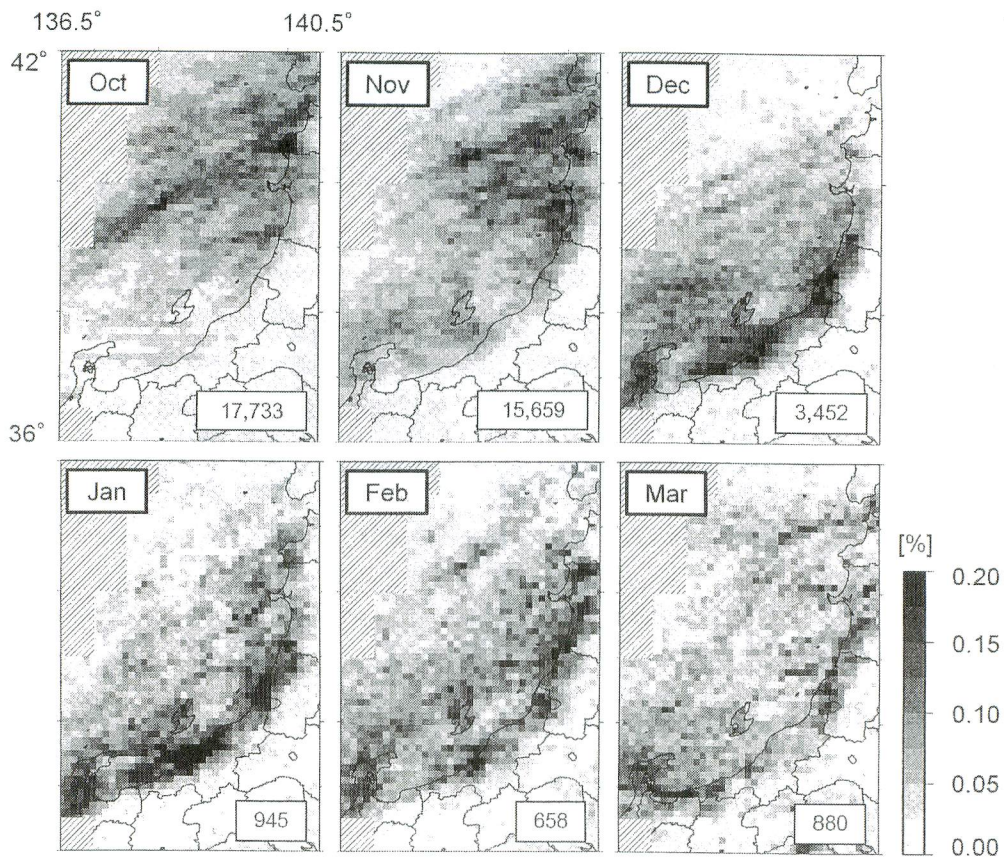


Fig. 2 Monthly lightning frequency map in the cold season, 1994-2011. Numbers written in the bottom-right corner represent annual mean lightning frequency [stroke/yr] in the study area.

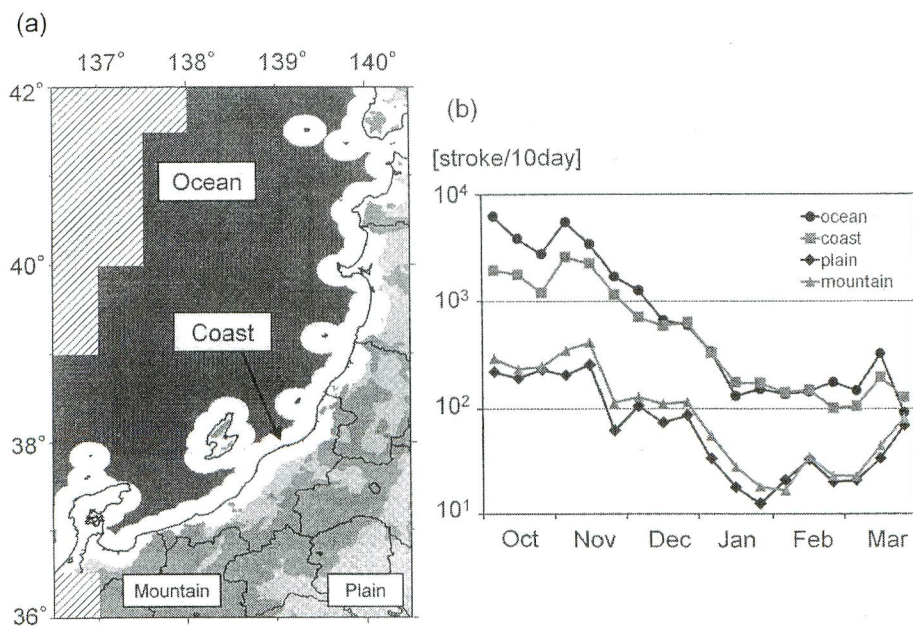


Fig. 3 Seasonal variation of lightning frequency in regions of various landforms (Ocean, Coast, Plain, Mountain). (a) Map showing the Ocean, Coast, Plain and Mountain region. (b) Seasonal variation of lightning frequency in each region.

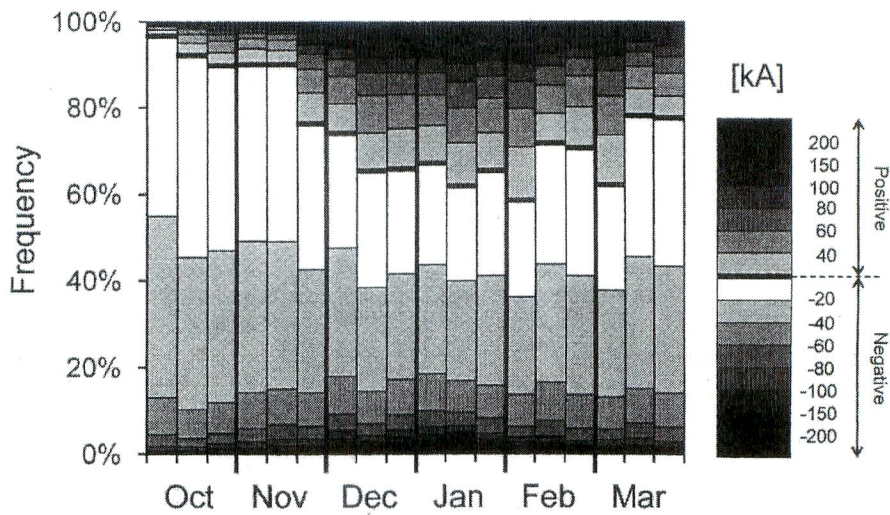


Fig. 4 Seasonal variation of lightning peak current in the study area. Minimum peak current of negative stroke and positive stroke are respectively -10 kA and 20 kA.

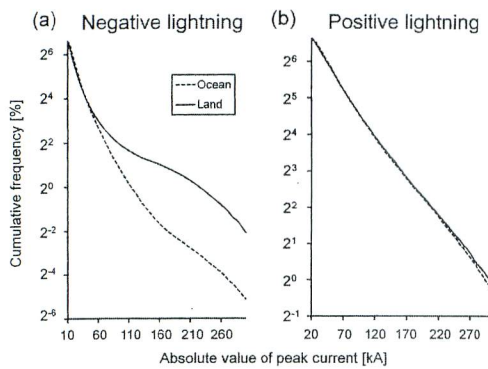


Fig. 5 Comparisons of cumulative frequency of lightning peak current [kA] between land and ocean area. (a) Negative lightning. (b) Positive lightning.

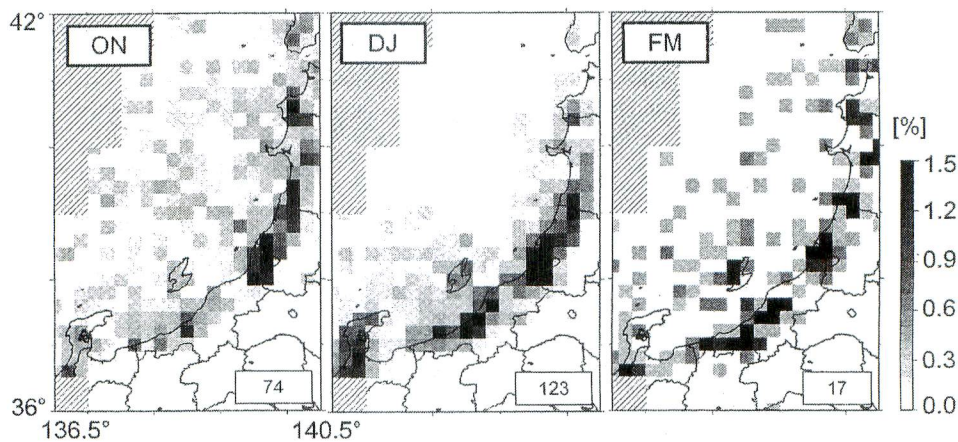


Fig. 6 Seasonal variation of negative high-current (peak current exceeds 180 kA) lightning frequency (ON : October-November, DJ : December-January, FM : February-March).

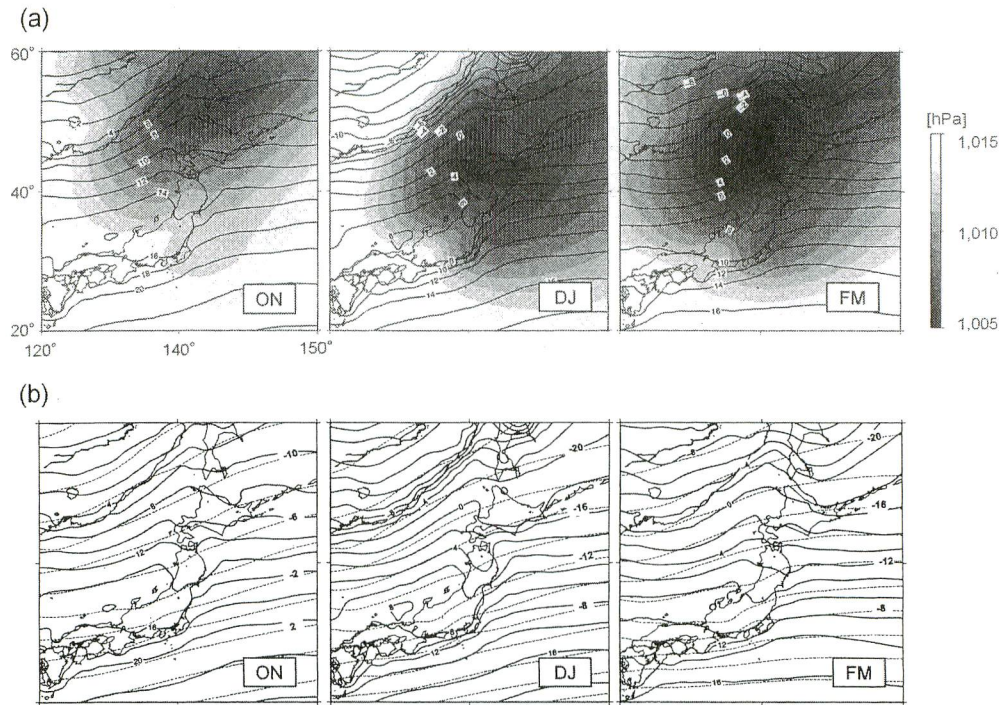


Fig. 7 Composites of several meteorological elements on the lightning days. (a) Sea-level pressure [hPa] and surface air temperature [°C]. (b) Air temperature [°C] at surface (solid line) and 700 ha pressure level (broken line).

Table 1 Number of selected lightning days and mean lightning frequency on the lightning days.

month	発雷日 (days)	日平均落雷頻度 (stroke/day)
Oct	144	2,664
Nov	170	2,029
Dec	140	656
Jan	52	417
Feb	36	453
Mar	52	407

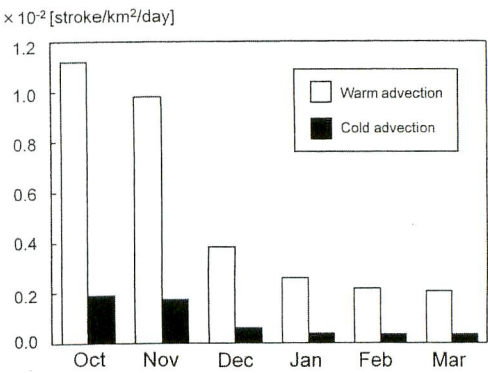


Fig. 9 Seasonal changes in daily mean stroke density [stroke/km²/day] observed in warm advection and cold advection area on lightning days.

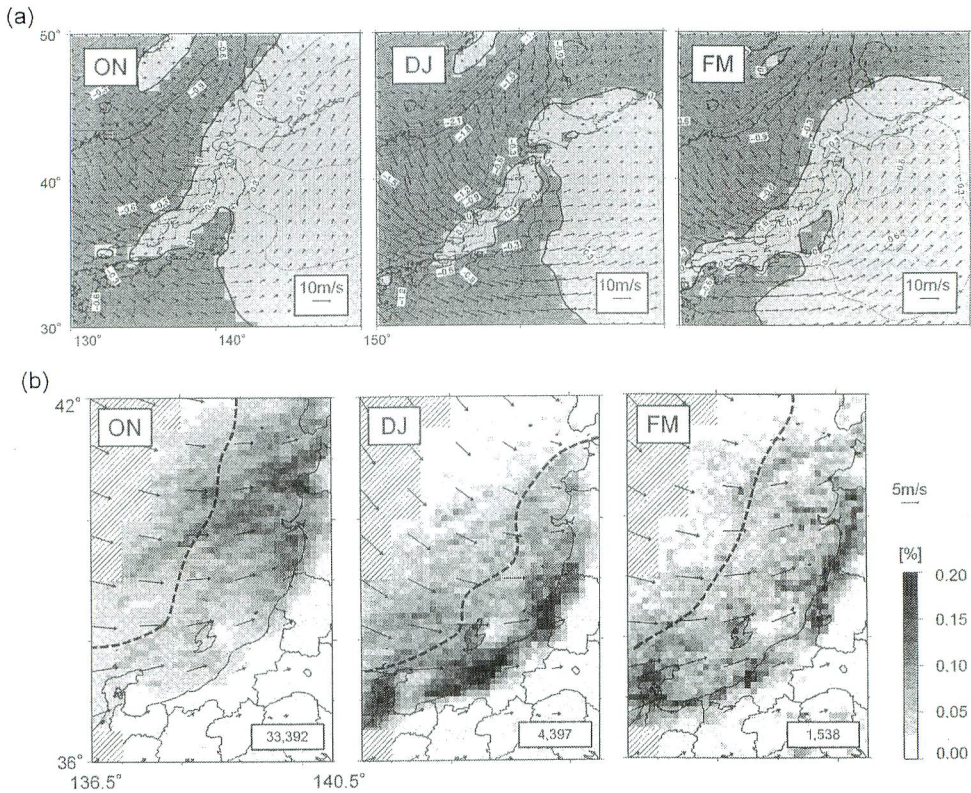


Fig. 8 Comparisons of surface horizontal temperature advection [$^{\circ}\text{C/hr}$] and wind vectors at surface level. (a) Composites of horizontal temperature advection [$^{\circ}\text{C/hr}$] and wind vectors at surface level. (b) Distributions of surface wind vectors, lightning frequency and boundary of warm advection and cold advection area (broken line).

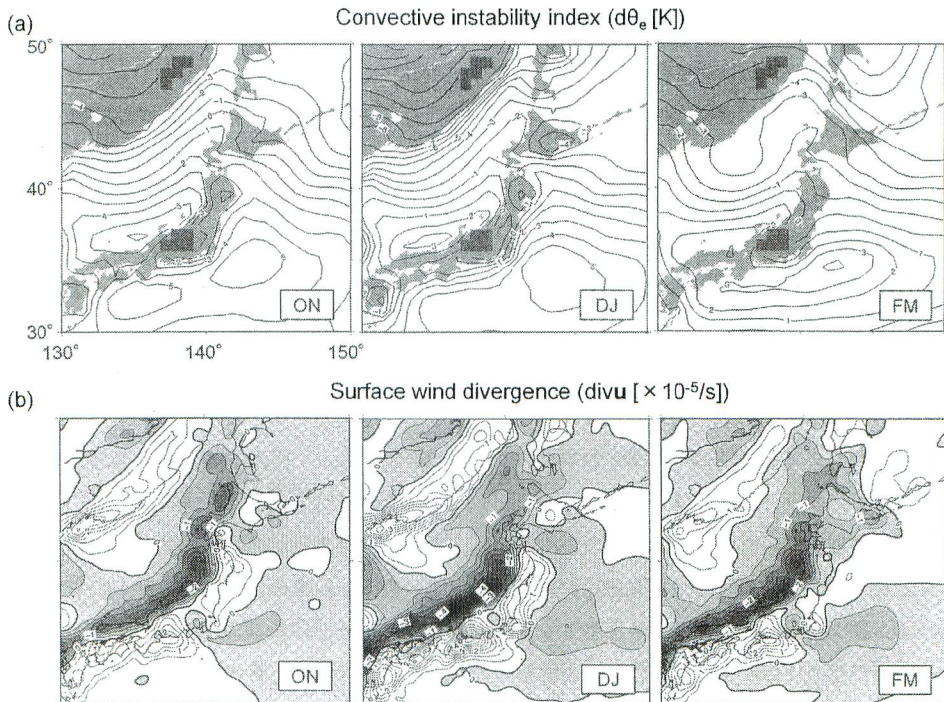


Fig. 10 Composites of convective instability index ($d\theta_e$ [K]) and surface wind divergence [$\times 10^{-5}/\text{s}$] on the lightning days. (a) Composites of $d\theta_e$ [K]. Shaded areas are the grid cells with altitudes exceeding 700 m. (b) Composites of surface wind divergence [$\times 10^{-5}/\text{s}$].

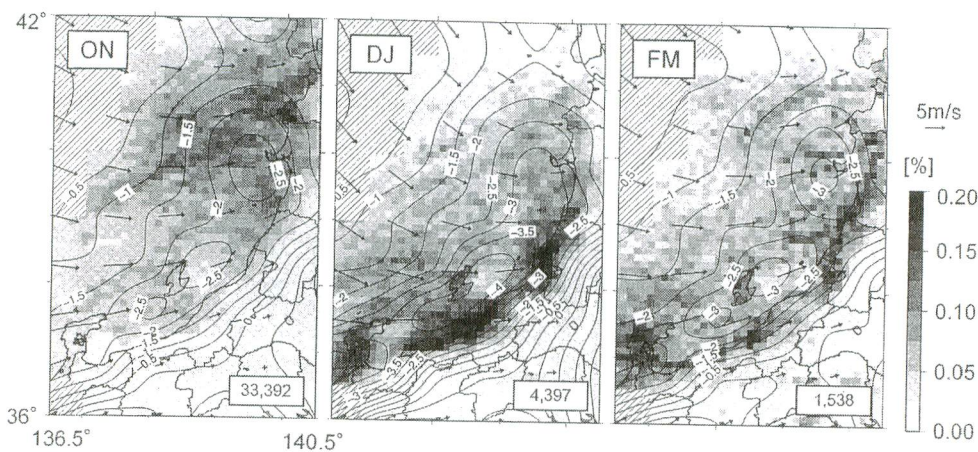


Fig. 11 Composites of surface wind vectors, wind divergence [$\times 10^{-5}/s$] and lightning frequency on the lightning days.

Table 2 Frequency of mean wind direction within the area, as shown in Fig. 12. The most frequent wind direction in each season is written in bold letters.

	Oct-Nov (%)	Dec-Jan (%)	Feb-Mar (%)
N	5.7	10.6	10.3
NE	1.6	2.5	1.9
E	1.1	0.7	1.3
SE	2.5	1.9	2.6
S	8.3	4.9	8.3
SW	24.5	15.0	22.4
W	28.4	23.6	35.9
NW	28.0	40.7	17.3
Total	100.0	100.0	100.0

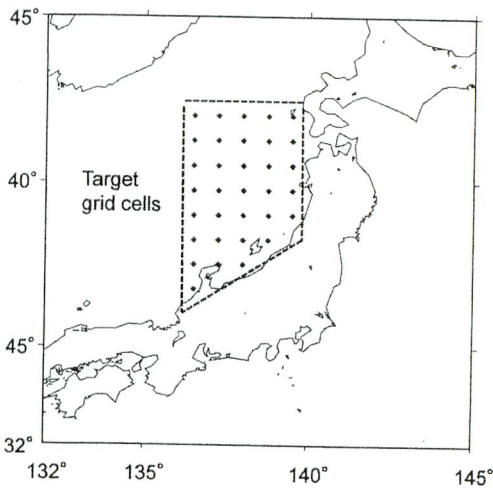


Fig. 12 Location of grid cells used for calculating mean wind vectors in the study area.

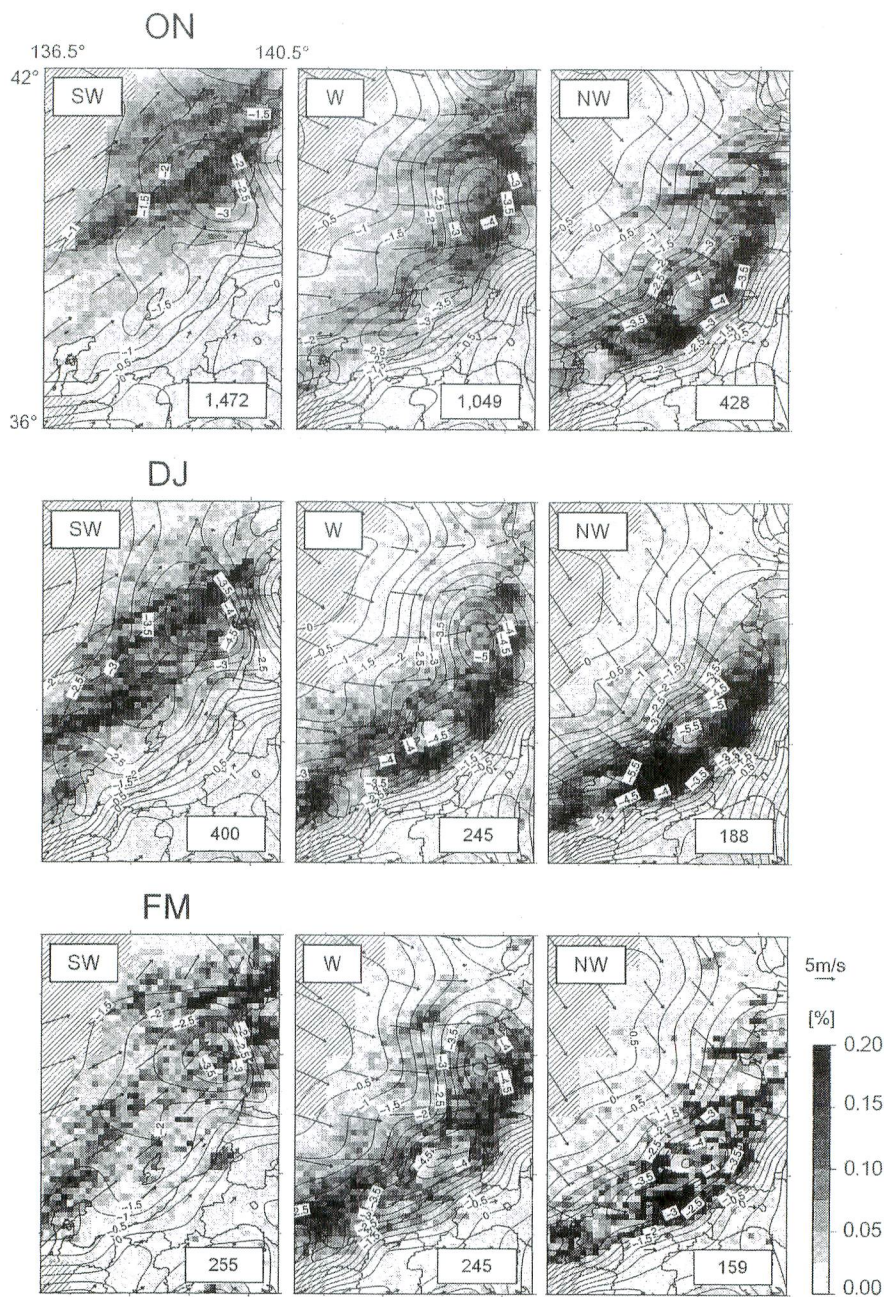


Fig. 13 Composites of lightning frequency, surface wind vectors and wind divergence [$\times 10^{-5}/s$] during time periods of SW, W and NW winds. Numbers written in the bottom-right corner represent mean lightning frequency [stroke/6 hr] of each group.

Reprinted from *Quarterly Jour. of Geography*. Vol. 65-4, pp. 189~206, 2014.